Sixth International Conference on Durability of Concrete Structures **Paper Number DSM08**
18 - 20 July 2018
University of Leeds, Leeds, West Yorkshire, LS2 9JT, United Kingdom

Meso-scale Fracture Modelling of Concrete Cover Induced by Non-uniform Corrosion of Reinforcing Bar

X. Xi and S. Yang
Department of Civil and Environmental Engineering, University of Strathclyde, Glasgow, UK

C. Li
School of Engineering, RMIT University, Melbourne, Australia

ABSTRACT

Corrosion-induced concrete cracking is a significant durability problem for reinforced concrete structures. In practice, critical corrosion degree to surface cracking and crack width evolution are of significance in regards to the assessment of serviceability of reinforced concrete structures. Literature review suggests that, although considerable research has been undertaken on corrosion-induced concrete cracking, little has been focused on non-uniform corrosion of reinforcing bar, especially by considering concrete as a three-phase materials. In this paper, a meso-scale fracture model, consisting of aggregates, cement paste/mortar and ITZ, is established. To simulate arbitrary cracking in concrete, cohesive elements are inserted in the fine meshes and the process is achieved through a script written in Python. It has been found that some microcracks occur before they are connected to form a dominating discrete crack approaching to the surface. The surface crack width is obtained as a function of corrosion degree and verification against experimental results from literature is conducted.

Keywords: non-uniform corrosion, meso scale model, cohesive crack model, mixed mode fracture

1.0 INTRODUCTION

Reinforced concrete (RC) structures have been the most common type of structures used in the civil engineering constructions (e.g., buildings, bridges, retaining walls, tunnels, piers.) RC structures will suffer from reinforcement corrosion in chloride (Cl^-) and carbon dioxide (CO_2) laden environment. Deterioration of RC structures induced by corrosion of reinforcement is the greatest threat to the durability and service life of civil engineering construction.

To model the corrosion induced cracking of concrete, some researchers have employed analytical method to predict time to surface cracking (Bhargava *et al.*, 2006; Liu and Weyers, 1998; Lu *et al.*, 2011), crack patterns (Bazant, 1979; Yang *et al.*, 2017a) and crack width development (Li, 2003; Li *et al.*, 2006), etc. However, most applications of analytical modelling in crack propagation in concrete are limited to homogeneous material, particular boundary conditions (i.e., thick-wall model), uniform corrosion and smeared crack assumption, etc. In fact, concrete is heterogeneous and concrete cover has structural effect on stress field of concrete. Moreover, due to the diffusion nature of chloride ingress from different sides of concrete, the corrosion process is seldom uniform along the reinforcing bar.

In light of the limitations of analytical modelling on crack propagation in concrete, some researchers have resorted numerical methods to model concrete cover cracking induced by reinforcement corrosion (Jang and Oh, 2010). For example, Chen and Leung (2015) simulated concrete cover cracking for non-uniform corrosion of single rebar, middle rebar and corner rebar by inserting cohesive elements into predefined crack paths and applying different displacement boundary conditions on two sides of models. Xi and Yang (2017) modelled the concrete cracking caused by non-uniform corrosion of multiple rebars and found short reinforcement spacing could cause delamination of the whole cover. In most of these models, concrete is considered as a homogenous material and its mechanical parameters are the same for the entire model. Almost all numerical models regarded corrosion induced cracking of concrete as tensile cracking (Chen and Leung, 2015; Šavija *et al.*, 2013; Xi and Yang, 2017; Yang *et al.*, 2017b) or combined tensile cracking and compression failure/damage (Jang and Oh, 2010) and the shear properties of concrete are not considered. However, acoustic emission experiments on corrosion-induced concrete cracking has indicated that contributions of mode I and mode II are varied during crack propagation and mechanism of crack propagation is mostly mode-I fracture with the minor contribution of mixed-mode and mode-II fractures (Farid Uddin *et al.*, 2004).

This paper attempts to develop a numerical model to simulate discrete crack propagation in heterogeneous concrete and predict the surface crack width under the non-uniform corrosion of reinforcement. A non-uniform corrosion model is first formulated as based on experimental results. Concrete is considered as three-phase (i.e., consisting of mortar, aggregates and ITZ) material, which is achieved by a Python script controling the drawings in AutoCAD. In order to model the arbitrary discrete cracking of concrete, cohesive crack elements are inserted into a sufficiently fine mesh for mortar, aggregates and ITZ separately, through an in-house script written in Python. The constitutive model of cohesive elements for mixed mode fracture is discussed. After the formulation of the model, an example is presented to demonstrate its application and some toughness mechanisms in cracking propagations are captured. The developed model is then verified by comparing the results with those from experiments.

2.0 NON-UNIFORM CORROSION MODEL

When the reinforcement in concrete is corroded, the corrosion products will accumulate and push the surrounding concrete outwards which cause cracking and delamination of RC structures. As shown in Fig. 1, Φ is the diameter of the reinforcing rebar and d_0 is the thickness of the annular layer of concrete pores at the interface between the bar and concrete, often referred to the "porous zone" or "corrosion accommodation zone". Usually d_0 is constant once concrete has hardened. It is assumed that no stress is produced and exerted on the concrete until the "porous zone" around the reinforcement is fully filled by the corrosion products. As the corrosion products proceed further in concrete, a band of corrosion products forms, as shown in Fig. 1(a). It has been found that the front of corrosion products for the half of rebar facing concrete cover is in a semi-elliptical shape, while corrosion of the opposite half of rebar is negligibly small and can be neglected (Yuan and Ji, 2009).As illustrated in Fig. 1(b), there may be three bands accommodating the corrosion products: the semi-elliptical band of corroded steel with maximum thickness $d_{co\text{-}st}$, the porous circular band d_0 and the semi-elliptical rust band with maximum thickness d_m (also referred to as corrosion expansion displacement in this paper). The front of the corrosion is in a semi-elliptical shape with the semi-major axis equal to $\phi/2+d_0+d_m$ and the semi-minor axis equal to $\phi/2+d_0$. By considering the original location of inner boundary of the concrete, i.e., $\phi/2+d_0$, the displacement boundary condition of the concrete structure can be derived as follows,

$$r=\frac{(\phi+2d_0+2d_m)(\phi+2d_0)}{\sqrt{(2\phi+4d_0)^2+16d_m(\phi+2d_0+d_m)\cos^2\theta}}-\frac{\phi}{2}-d_0 \qquad (1)$$

where $0\le\theta\le\pi$.

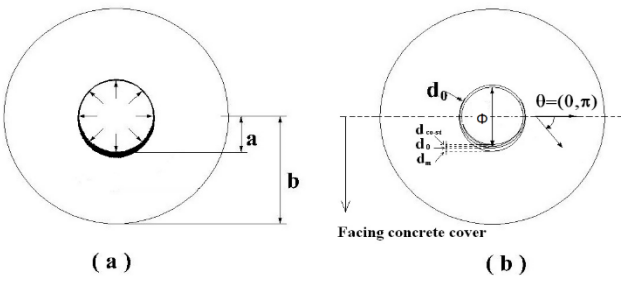

Fig. 1. Semi-elliptical corrosion model

3.0 CONCRETE CRACK MODEL

3.1 Meso-scale Discrete Crack Model of Concrete

In this paper, concrete is modelled as a three-phase (i.e., consisting of mortar, aggregates and ITZ) material. The aggregate size distribution can be represented by a grading curve, which is usually expressed in terms of cumulative percentage passing through a series of sieves with different opening sizes. A typical gradation of aggregate size distribution is listed in Table 1. For simplicity, only coarse aggregates larger than 2.4 mm are modelled in this study, while fine aggregates and cement are treated as mortar phase. Coarse aggregates generally occupy 40% of the whole volume of concrete. The basic idea of meso-scale model is to generate and place aggregates in a repeated manner until the target area is fully packed by aggregates. Firstly, an aggregate is generated with 3-7 sides and a random size in specified grading segments. Then the aggregate is placed in the target area with random position. There is a minimum distance between aggregates and boundary. More aggregates are generated and placed one by one until total fraction of aggregates in the grading segments reaches the specified value. There is no overlapping of aggregates in the placing process. The remaining area becomes the target area for next smaller grading segments and the procedures are repeated until the last aggregate of smallest size is generated and placed. The script for producing the three-phase structure is written in Python which controls the drawings in AutoCAD; the structure is then imported into FE software (i.e., ABAQUS) for analysis.

To model arbitrary cracking in concrete, the cohesive elements are embedded at the interfaces throughout the mesh; very fine mesh is produced to ensure random crack paths. The insertion process of cohesive elements is shown in Fig. 2. First, all individual nodes are replaced by certain number of new nodes at the same location. The number of

Table 1. Three-segment gradation of aggregate size distribution

Aggregate size (mm)	Fraction (%)
2.40-4.76	20.2%
4.76-9.52	39.9%
9.52-19.05	39.9%

newly created nodes depends on the number of the elements connecting to the original node. Second, the newly created nodes at the interface between two triangle elements are identified and linked to form a cohesive element. The cohesive elements are shown in red in Fig. 2. The insertion process of cohesive elements is accomplished by an in-house script written in Python. Figure 3 shows the inserted cohesive elements at the interface of aggregate and mortar, as well as in the aggregates and the mortar. Therefore, the developed model is capable of simulating crack propagation both at the interface and in the bulk mortar and aggregates, depending on their material properties.

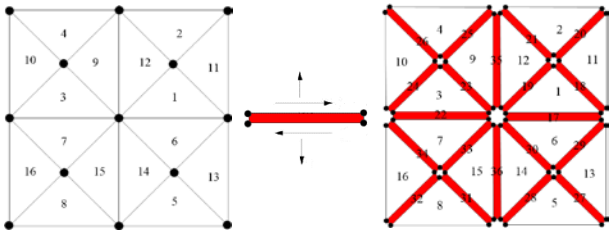

(a) (b) (c)

Fig. 2. Insertion process of cohesive elements: (a) initial mesh; (b) inserted cohesive element based on newly created nodes; and (c) mesh after insertion of cohesive elements

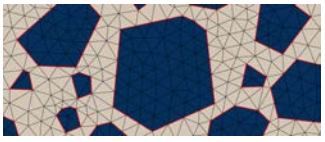

Interfacial cohesive elements between aggregates and mortar

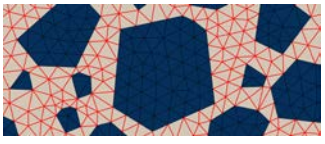

Cohesive elements in mortar

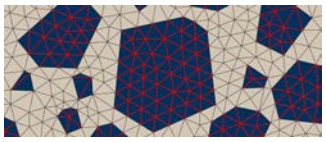

Cohesive elements in aggregates

Fig. 3. Inserted cohesive elements in the FE mesh

3.2 Mixed Mode Fracture Model

Due to complex loading condition, materials heterogeneous and aggregate interlocking etc., in most cases, cracks in concrete propagate under mixed-mode conditions rather than isolated mode-I or mode-II. Camanho *et al.* proposed a coupled model by considering variation fracture toughness under different mode ratios, which has been employed into the commercial software ABAQUS (Camanho *et al.*, 2002).

Figure 4 illustrates the response model for mixed-mode fracture. It can be seen that, before damage initiation, the normal, shear and effective stresses will increase linearly by a slope of penalty stiffness. When the effective displacement increases to the elliptical with semi-major axis δ_s^0 and semi-minor axis δ_n^0, the damage initiated and then the stresses begin decreases. The mixed-mode fracture energy varies with mixed ratio or contribution of shear on fracture. The effective relative displacement to completely failure varies from completely failure displacement for mode-I to that of mode-II.

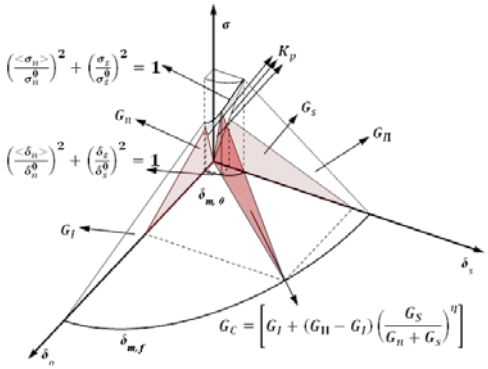

Fig. 4. Mixed mode fracture constitutive model

If the shear and tensile strength are the same and fracture energies for pure mode-I and mode-II are also the same, the ellipse to damage initiation becomes a circle with strength value as the radius. Moreover, the mixed-mode fracture energy is equal to pure mode fracture and the effective relative displacement to completely failure will not change with the mixed-mode ratio.

4.0 WORKED EXAMPLE AND VERIFICATION

Figure 5 shows the mesh of the meso-scale RC cover structure with a middle rebar. The size of the RC structure is set 150×150 mm and the thickness of concrete cover is 40 mm. The average size of elements in the mesh is about 1.6mm, which is very fine to simulate arbitrary cracks. The boundary condition to the concrete cylinder caused by corrosion is first calculated from the non-uniform corrosion model mentioned above.

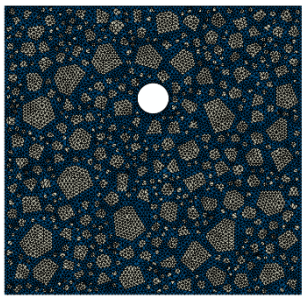

Fig. 5. Mesh for the worked example

Table 2. Values for geometric and mechanical parameters for different phases (Rao and Raghu Prasad, 2004; Ren *et al.*, 2015; Tregger *et al.*, 2006)

Description	Symbol	Values
Cover thickness	C	40 mm
Diameter of steel bars	D	16 mm
Young's modulus of aggregate	E_{Agg}	70 GPa
Young's modulus of mortar	E_{Mor}	25 GPa
Poisson's ratio of aggregate	υ_{Agg}	0.2
Poisson's ratio of mortar	υ_{Mor}	0.2
Tensile strength of mortar	$\sigma_{n,Mor}$	2.6 MPa
Tensile strength of ITZ	$\sigma_{n,ITZ}$	1.3 MPa
Shear strength of mortar	$\sigma_{s,Mor}$	2.6 MPa
Shear strength of ITZ	$\sigma_{s,ITZ}$	1.3 MPa
Mode I fracture energy of mortar	$G_{I,Mor}$	40 N/m
Mode I fracture energy of ITZ	$G_{I,ITZ}$	17 N/m
Mode II fracture energy of mortar	$G_{II,Mor}$	80 N/m
Mode II fracture energy of ITZ	$G_{II,ITZ}$	34 N/m

As a demonstration of the application of the developed numerical method and techniques in solving non-uniform corrosion induced concrete cracking, an example is carried out. The values for all the basic parameters are shown in Table 2, together with their sources. As introduced in previous studies (Ren *et al.*, 2015), the shear fracture properties are hard to identify due to the lack of experimental data. Some researchers assumed the shear properties are the same as the normal ones (i.e., $\sigma_n^0 = \sigma_s^0$ and $G_I = G_{II}$). Some researchers proposed shear properties have little effect on corrosion induced concrete cracking and only mode-I fracture is considered in their model. For heterogeneous model with rough fracture surfaces, it is necessary to consider the effect of shear properties on concrete cracking. Experimental results on concrete indicated that the shear strength is greater or equal than tensile strength and the fracture energy for mode II is greater than that of mode I (Lens *et al.*, 2009). Thus, the shear strength are assumed the same with tensile strength and the fracture energy for model II is twice as much as that for mode I. Another important aspect for meso scale fracture modelling of concrete is the fracture properties of ITZ. Experimental results indicated that the tensile strength of ITZ is about 1/16 to 3/4 times of strength of mortar matrix (Rao and Raghu Prasad, 2004; Tregger *et al.*, 2006). So the tensile strength of ITZ is given as 0.5 times of tensile strength of mortar matrix. Further, it is assumed that the facture energy for ITZ is 0.013 times of value of tensile strength of ITZ (Rao and Raghu Prasad, 2004). The shear strength of ITZ is assumed the same as tensile strength of ITZ and the fracture energy for mode II is two times as much as that of mode II. The mechanical properties of aggregates are normally considerably stronger than mortar and the ITZ; thus it is in general very rare to have a crack breaking through an aggregate. In this paper, fracture properties are only assigned in the ITZ and mortar to simulate cracking, in light of reducing computational cost.

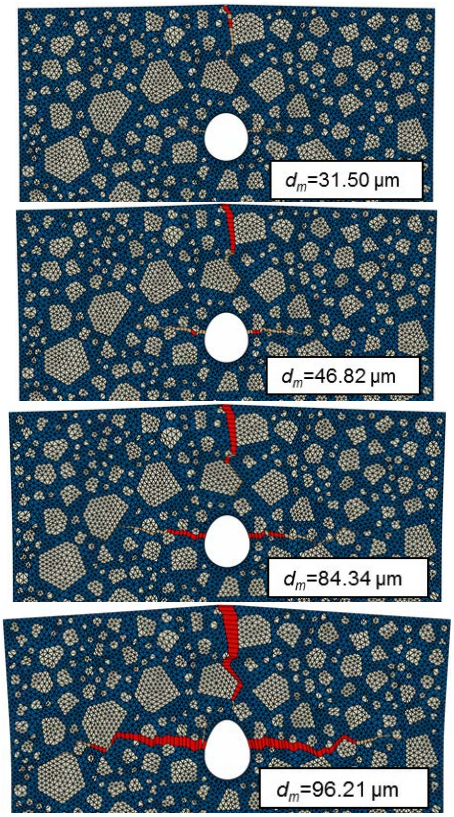

Fig. 6. Crack propagation of concrete induced by non-uniform corrosion of reinforcement

Figure 6 shows the crack propagation process induced by non-uniform corrosion of reinforcement. Cohesive elements with damage variable D equal to 1 (i.e. complete failure) are plotted in red. It can be found that a few micro cracks are first initiated at the aggregate-mortar interfaces near the top surface of the concrete cover. As corrosion continues, the micro cracks are then connected to form a dominant crack propagating from the concrete surface to the rebar. The phenomenon that a crack propagates from concrete surface towards the reinforcement has a good agreement with the experiments (Caré *et al.*, 2009).With the maximum corrosion displacement increasing, two cracks appear in the two sides of

concrete cover. Unlike macro-scale fracture modelling which considers concrete as a homogeneous material (Xi and Yang, 2017), micro cracks always start first at the ITZ before they are connected and form a macro discrete crack. This is because the strength and fracture energy of ITZ cohesive elements are significantly lower than those of mortar.

Figure 7 illustrates the mircocrack shielding, crack deflection and aggregate bridging phenomena when cracks propagating in concrete. There are many microcracks appear near the stress concentration area. Some of the microcracks will propagate, connect and form a discrete or main crack. Crack deflection occurs when the path of least resistance is around a strong aggregate or a weak interface. Aggregate bridging occurs the crack propagating along two sides of aggregate interface and advancing beyond the aggregate. As such, the developed meso-scale fracture model is advantageous compared with most existing concrete fracture models (Chen and Leung, 2015) in terms of capturing toughening mechanisms and crack propagation.

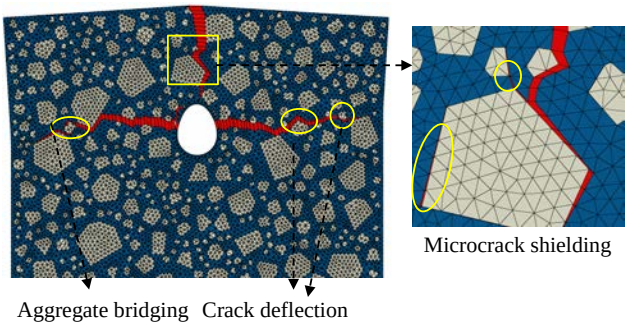

Fig. 7. Some toughening mechanisms in crack propagation process

For the heterogeneous concrete model, the aggregates are randomly generated but following the same volume fraction, grading, size, etc. Figure 8 illustrates the top surface crack development with maximum corrosion displacement. It can be found that, surface crack width of concrete cover initiates when increases to about 0.03 mm and then near linearly increases. The meso scale randomness has little effect on surface crack initiation. While the long-term crack width is affected by randomness which is reasonable because the aggregate distribution will affect the mix mode fracture energy and the crack morphology has effect on crack width. For example, model 02 has the smallest surface crack width in Fig. 8 because the contribution of shear on top crack is greater. In general, the meso scale fracture model in this study has a good repeatability.

To verify the proposed numerical method, the results are compared with experimental results from Andrade *et al*. (1993). According to the literature

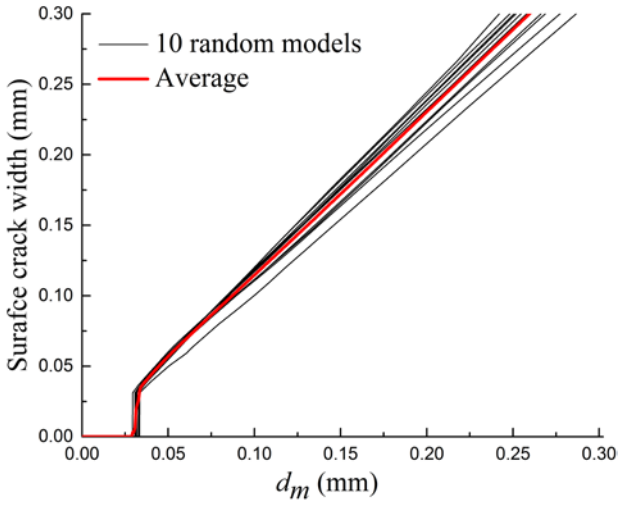

Fig. 8. Surface crack width as a function of corrosion expansion displacement for 10 meso scale models

searched, most experimental test data are based on based on uniform corrosion development by electric current method for accelerated corrosion. The meso-scale fracture model is able to simulate uniform corrosion induced concrete cracking. The tensile strength of concrete samples in the experiments (Andrade *et al.*, 1993) is about 3.55 MPa. According to the meso scale numerical modelling of direct tensile tests on concrete (Ren *et al.*, 2015), the basic parameters are presented in Table 3. It should be noted that, the thickness of “porous zone” between concrete and rebar is considered as 12.5 μm in the numerical results. The experimental results of crack width were expressed as a function of the radius loss of rebar. For the sake of comparison with the numerical results, the uniform corrosion displacement is transformed to radius loss of rebar.

Table 3. Values used for comparison and validation (Andrade *et al.*, 1993; Ren *et al.*, 2015)

Description	Values
Cover thickness	20 mm
Diameter of steel bars	16 mm
Tensile strength of concrete	3.5 MPa
Young’s modulus of aggregate	70 GPa
Young’s modulus of mortar	25 GPa
Poisson’s ratio of aggregate	0.2
Poisson’s ratio of mortar	0.2
Cohesive strength of mortar	6 MPa
Cohesive strength of ITZ	2 MPa
Fracture energy of mortar	60 N/m
Fracture energy of ITZ	30 N/m

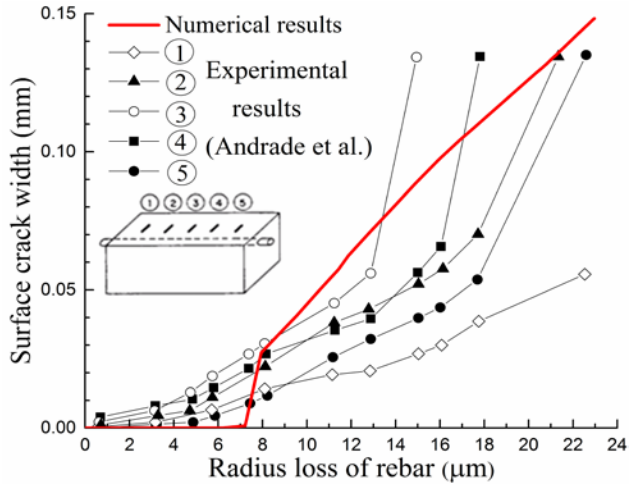

Fig. 9. Experimental verification of the crack width

The relationship between uniform corrosion displacement and radius loss of rebar can be expressed as follows:

$$d_{m,u} = \left(\frac{\rho_{st}}{\rho_{rust} \times \alpha_{rust}} - 1 \right) \times \Delta R - d_0 \quad (2)$$

The comparisons of the crack width from the developed numerical model and the experiments are illustrated in Fig. 9. It can be found that the progress of crack width simulated is in reasonably good agreement with the experimental results.

5.0 CONCLUSION

In this paper, a numerical model has been developed to simulate discrete crack propagation in heterogeneous concrete and predict the surface crack width under the non-uniform corrosion of reinforcement. A non-uniform corrosion model based on experimental results was first formulated. Three phases (i.e., mortar, aggregate and ITZ) heterogeneous concrete model was created by a script written in Python. To model the arbitrary cracking of concrete, cohesive crack elements were inserted into very fine meshes of aggregate, mortar and ITZ separately. The constitutive model of cohesive elements for mixed mode fracture was discussed. A worked example was presented to demonstrate the derived model and the repeatability of the model was verified. Some meso-scale toughness mechanisms of concrete cracking (e.g., microcracks shielding, crack deflection, aggregate bridging and crack overlap.) were captured. Then comparisons of numerical results with experimental results from literature were made. It has been found the numerical results are in good agreement with the experimental results.

Acknowledgement

Financial support from European Commission via the Marie Sklodowska-Curie H2020 RISE scheme under 645696 is gratefully acknowledged.

References

Andrade, C., Molina, F.J., Alonso, C., 1993. Cover cracking as a function of rebar corrosion: Part 1-experiment test. Materials and Structures, 26: 453-454.

Bazant, Z.P., 1979. Physical model for steel corrosion in concrete sea structures - theory. Journal of the Structural Division-ASCE, 105(6): 1137-1153.

Bhargava, K., Ghosh, A.K., Mori, Y., Ramanujam, S., 2006. Model for cover cracking due to rebar corrosion in RC structures. Engineering Structures, 28(8): 1093-1109.

Camanho, P.P., Davila, C.G., Moura, M.F.d., 2002. Numerical Simulation of Mixed-Mode Progressive Delamination in Composite Materials. Journal of Composite Materials-ASCE, 34(16): 1415-1438.

Caré, S., Nguyen, Q.T., Beddiar, K., Berthaud, Y., 2009. Times to cracking in reinforced mortar beams subjected to accelerated corrosion tests. Materials and Structures, 43(1-2): 107-124.

Chen, E., Leung, C.K.Y., 2015. Finite element modeling of concrete cover cracking due to non-uniform steel corrosion. Engineering Fracture Mechanics, 134: 61-78.

Farid Uddin, A.K.M., Numata, K., Shimasaki, J., Shigeishi, M., Ohtsu, M., 2004. Mechanisms of crack propagation due to corrosion of reinforcement in concrete by AE-SiGMA and BEM. Construction and Building Materials, 18(3): 181-188.

Jang, B.S., Oh, B.H., 2010. Effects of non-uniform corrosion on the cracking and service life of reinforced concrete structures. Cement and Concrete Research, 40(9): 1441-1450.

Lens, L.N., Bittencourt, E., d'Avila, V.M.R., 2009. Constitutive models for cohesive zones in mixed-mode fracture of plain concrete. Engineering Fracture Mechanics, 76(14): 2281-2297.

Li, C.Q., 2003. Life-cycle modelling of corrosion-affected concrete structures: Propagation. Journal of Structural Engineering-ASCE 129(6): 753-761.

Li, C.Q., Melchers, R.E., Zheng, J.J., 2006. Analytical model for corrosion-induced crack width in reinforced concrete structures. ACI Structural Journal, 103(4): 479-487.

Liu, Y., Weyers, R.E., 1998. Modelling the time-to-corrosion cracking in chloride contaminated reinforced concrete structures. ACI Materials Journal, 95(6): 675-681.

Lu, C., Jin, W., Liu, R., 2011. Reinforcement corrosion-induced cover cracking and its time prediction for reinforced concrete structures. Corrosion Science, 53(4): 1337-1347.

Rao, G.A., Raghu Prasad, B.K., 2004. Influence of type of aggregate and surface roughness on the interface fracture properties. Materials and Structures, 37(5): 328-334.

Ren, W., Yang, Z., Sharma, R., Zhang, C., Withers, P.J., 2015. Two-dimensional X-ray CT image based meso-scale fracture modelling of concrete. Engineering Fracture Mechanics, 133: 24-39.

Šavija, B., Luković, M., Pacheco, J., Schlangen, E., 2013. Cracking of the concrete cover due to reinforcement corrosion: A two-dimensional lattice model study. Construction and Building Materials, 44: 626-638.

Tregger, N., Corr, D., Graham-Brady, L., Shah, S., 2006. Modeling the effect of mesoscale randomness on concrete fracture. Probabilistic Engineering Mechanics, 21(3): 217-225.

Xi, X., Yang, S., 2017. Time to surface cracking and crack width of reinforced concrete structures under corrosion of multiple rebars. Construction and Building Materials, 155: 114-125.

Yang, S., Li, K., Li, C.Q., 2017a. Analytical model for non-uniform corrosion-induced concrete cracking. Magazine of Concrete Research: 1-10.

Yang, S.T., Li, K.F., Li, C.Q., 2017b. Numerical determination of concrete crack width for corrosion-affected concrete structures. Computers & Structures, in Press.

Yuan, Y., Ji, Y., 2009. Modeling corroded section configuration of steel bar in concrete structure. Construction and Building Materials, 23(6): 2461-2466.